YF-16 Inlet Design and Performance

J.E. Hawkins*
General Dynamics' Fort Worth Division, Fort Worth, Texas

The YF - 16 inlet design, the integration of airframe and inlet, the design philosophy, development tests, and performance of the inlet throughout the flight and maneuver envelope of the airplane are reviewed. Model data are included which show the airplane forebody effect on the inlet flowfield and the performance of the inlet in terms of pressure recovery, distortion, turbulence, inlet stability, and spillage drag. The data presented verify that the single, fixed-geometry, normal-shock inlet located in the protective flowfield of the fuselage nose provides an integrated inlet/airframe configuration that meets all of the design and performance goals established for the YF - 16 air-combat fighter. Indeed, the simple, low-cost, and uncomplicated inlet design optimizes rather than compromises airplane performance in the air-combat arena, and at the same time provides a Mach 2 capability for the airplane.

Introduction

THE YF - 16 airplane is a prototype multirole tactical fighter built by General Dynamics' Fort Worth Division under Air Force Contract F33657-72-C-0702. The airplane is powered by a single Pratt & Whitney F100-PW-100 engine, which is identical to that used in the F-15. The YF-16 primary mission is air superiority in the subsonic and transonic regions to Mach 1.6, with a dash capability to Mach 2.0.

Inlet design studies for the lightweight fighter concept, initiated in 1971 under a contract with Aeronautical Systems Division (ASD), "Study to Validate Expanded Energy-Maneuverability Through Trade-Off Analysis," led to the selection of a simple, fixed-geometry, normal-shock inlet design and underbelly inlet location. The design concept was proven in one wind-tunnel test entry before award of the lightweight fighter prototype contract in April 1972. The design was further developed and the performance substantiated and completely documented in two subsequent wind-tunnel test entries. All tests were accomplished over a 13-month period in only 217 wind-tunnel hrs.

This paper reviews the inlet design requirements and philosophy; the inlet design, including the integration of airframe and inlet; the development test program; and the performance of the inlet throughout the flight and maneuver envelope of the airplane.

Requirements

Specific criteria used for the design and location of the inlet and for evaluating inlet performance in terms of pressure recovery, drag, and inlet/engine compatibility were as follows:

1. Maximum usable maneuver/energy potential (high inlet total pressure recovery and low spillage drag) in the air-combat arena from Mach 0.6 to 1.6 with emphasis on the region from Mach 0.8 to 1.2.
2. No restrictions on aircraft operation due to inlet and engine incompatibility; this includes snap power-lever operation at limit values of angles of attack and sideslip.
3. A maximum speed capability of about Mach 2, but without undue compromise to performance or stability of operation in the air-combat arena.
4. Minimum weight as a means of meeting performance and low-cost goals.
5. Minimum complexity to achieve low weight, low cost, and high reliability.

Presented as Paper 74-1062 at the AIAA/SAE 10th Propulsion Conference, San Diego, Calif; Oct. 21-23, 1974; submitted Dec. 2, 1974; revision received Aug. 21, 1975.

Index categories: Aircraft Configuration Design; Aircraft Testing; Airbreathing Propulsion, Subsonic and Supersonic.

*Project Propulsion Engineer, Aerospace Technology.

Early estimates of the airplane's α and β limits were established empirically. These original predictions are shown in Fig. 1 as the nominal maneuver envelopes (bounded by the solid lines). A more realistic estimate of the airplane's α and β limits were provided later by the YF-16 flight simulator, in which the flight characteristics were based on wind-tunnel test data, airplane weight distribution, and control response characteristics. The boundary of the shaded area in Fig. 1 is an envelope of α and β excursions produced by the simulator for rolling pullouts between maximum positive and maximum negative g. The rolls were initiated by simultaneous application of the stick force for a maximum roll command and that for a given pitch g command. Except for the power-approach condition, the rolls were continued through 360°, and then the roll rate was reduced to zero. In power approach a roll and stop maneuver to approximately 60° bank angle was simulated. The maximum negative α is based on a maximum roll maneuver combined with a -2.5 g pushover. Although this maneuver would be encountered infrequently in the "real world," it is within the control capability of the YF-16. From these estimates of airplane capability, inlet model test limits were established as shown by the dashed line in Fig. 1.

The inlet was designed to match the F100-PW-100 engine airflow characteristics, which are shown in Fig. 2. The engine control system limits the maximum noninal-engine corrected air-flow to standard-day values; this includes nonstandard-day conditions. A 3% tolerance allows for engine-to-engine variations. For inlet design purposes, the minimum engine airflow was established as the hot-day idle airflow. The engine control contains an idle-speed lockout feature that limits the minimum engine speed and airflow to intermediate power values above about Mach 1.4.

The requirements on engine-face pressure distortion were defined by the engine manufacturer in terms of instantaneous distortion indices KA2 (fan) and KC2 (high compressor). For the purpose of making a preliminary assessment of compatibility and of selecting worst-case test points so as to perform a more rigorous compatibility analysis, limiting values of KA2 and KC2 were given as a function of engine corrected airflow. Generally, the fan has been shown to be the limiting component for YF-16 inlet distortion patterns.

Inlet Description

The design features of the inlet are shown in Fig. 3. The inlet is a single, fixed-geometry, normal-shock configuration, located on the underside of the fuselage approximately 13 ft from the nose of the airplane. This inlet location provides a uniform flowfield at all combinations of α and β within the maneuver envelope, and also provides fuselage shielding to enhance maneuverability, i.e., no degradation in pressure recovery to 30° α and stable operation to 40° α subsonically,

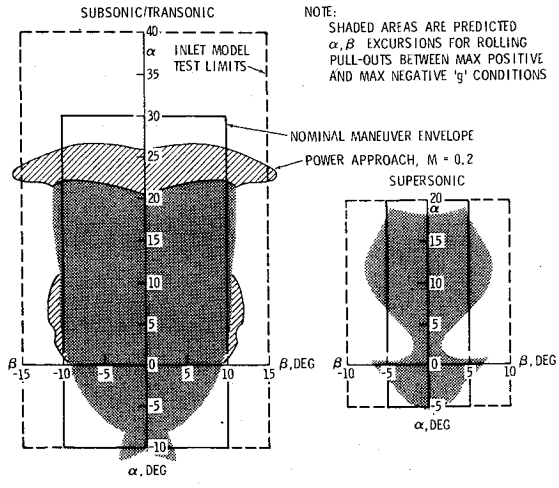

Fig.1 Predicted α and β limits.

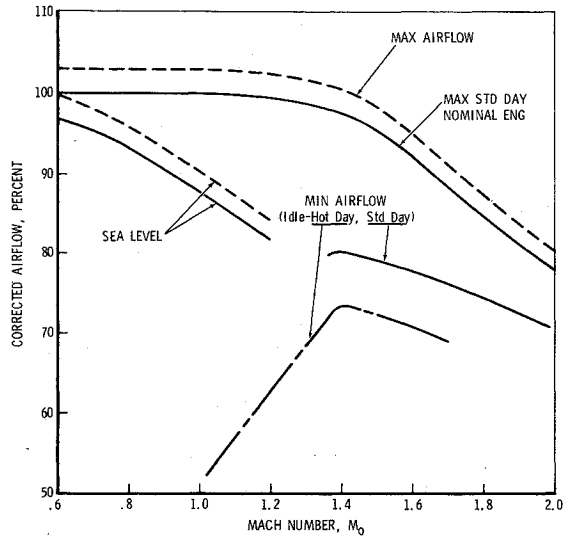

Fig.2 F100 engine airflow characteristics.

with an increase in pressure recovery with α at supersonic speeds. In addition, it isolates the inlet with respect to the gun to avoid gun-gas ingestion, and places the inlet forward of the nose gear to minimize foreign object ingestion.

The inlet cowl features a moderately blunt lower cowl lip that transitions by large corner radii into a sharp leading-edge extension or splitter-plate at the upper outboard corners. The splitter-plate leading-edge extends 10 in. ahead of the lower cowl lip to isolate the inlet normal shock from the fuselage boundary-layer air. This relatively short splitter-plate effectively isolates the inlet shock from the fuselage at all flight conditions and engine airflows. Also, its shortness minimizes boundary-layer buildup on the splitter, which, in turn, minimizes separation induced by shock/boundary-layer interaction and precludes the need for boundary-layer bleed on the splitter plate.

The splitter plate is curved to follow the body contour, but with a slightly greater radius of curvature, in order to provide efficient diversion of the fuselage boundary-layer air to the outside above the splitter plate and not into the inlet. The standoff distance of the splitter leading edge from the lower fuselage surface is 3.3 in. at the fuselage centerline. The wedge angle of the splitter plate on the inlet side is 5° from a waterline plane.

The design also features a thin, centerline, airfoil-shaped tension strut member inside the cowl, which minimizes cowl deflections under load and allows a lighter and less costly structural design. Duct flow quality is not affected by the strut. Blow-in-doors are located on the top side of the inlet on

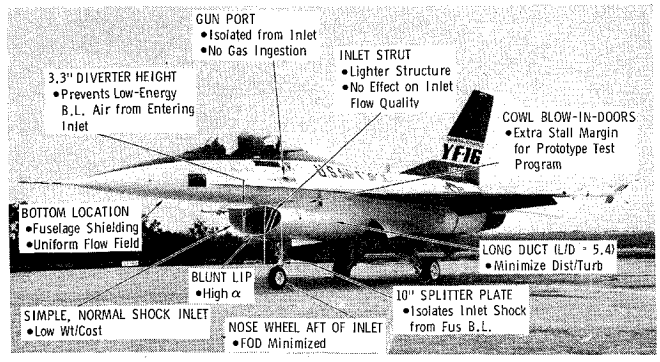

Fig.3 YF-16 prototype no. 1 – inlet design features.

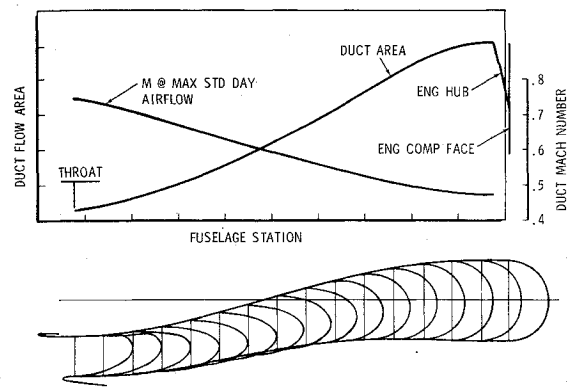

Fig.4 Subsonic duct geometry and area distribution.

either side of a diverter separating the inlet from the fuselage. These doors provide additional inlet flow area and extra stall margin during takeoff and landing.

The diverter begins 7 in. aft of the splitter-plate leading edge with an initial half-angle of 8°. A minimum flow divergence angle adjacent to the diverter of 1½° is provided in the diverter channel to efficiently channel the boundary-layer air past the inlet, with minimum drag and mimimum boundary-layer buildup ahead of the inlet because of the creation of an adverse pressure gradient. Small secondary air inlets, which supply air to the environmental control system air-to-air heat exchangers, are located on either side of the diverter well aft of the primary inlet lip (Fig. 3). These locations provide very-high-pressure-recovery air for the ECS and insure no interaction between the primary and secondary inlets. Secondary inlet size and drag are minimized.

The relatively long subsonic duct is a key element of the inlet system. Duct geometry and flow area distribution are shown in Fig. 4. The duct length from the inlet throat to the engine compressor face is approximately 5.4 times the engine compressor-face diameter. The gradual area expansion gives a near linear Mach number change from the throat to the compressor face to reduce diffuser losses. The fixed-inlet throat is sized to accommodate the maximum engine corrected airflow (nominal plus 3%) at a throat Mach number of 0.75, based on geometric throat area and assuming zero total pressure loss from freestream to the throat. The 5° splitter-plate ramp angle and the blunt cowl lip provide a contraction ratio of 1.16 from the inlet highlight area (capture area) to the inlet throat. The blunt lip with its attendant high contraction ratio was selected to prevent lip flow separation and resulting high distortion during airplane maneuvers to very high angles of attack. The blunt lip also increases lip suction to minimize spillage drag at subsonic and transonic flight speeds.

A unique built-in design feature of the YF-16 is the modular inlet concept, which allows easy removal of the first 93 in. of the inlet/nacelle assembly, thus providing a capability for enlarging the inlet to accommodate engine airflow growth or for incorporating a variable-geometry inlet for airplane speed

Table 1 Normal shock is optimum inlet type

Inlet Type	ΔA_i	Δ Dry Weight lb	Δ Mission Weight	Δ $\dot{\theta}$ M0.9	Δ $\dot{\theta}$ M1.2	Δ Accel Time (M0.9-1.5)	1-g P_s M0.9/30K'	1-g P_s M1.6/40K'	Max Mach
NORMAL SHOCK	0	0	0	0	0	0	0	0	2.0
FIXED RAMP OR SPIKE w/BYPASS (M_{DES} = 2.0)	+30%	+250	+4%	-2%	-7%	+12%	-6%	+1.5%	2.0
VARIABLE GEOMETRY (M_{DES} = 2.2)	+13%	+250	+3%	-2%	-7%	+4%	-6%	+13%	2.2

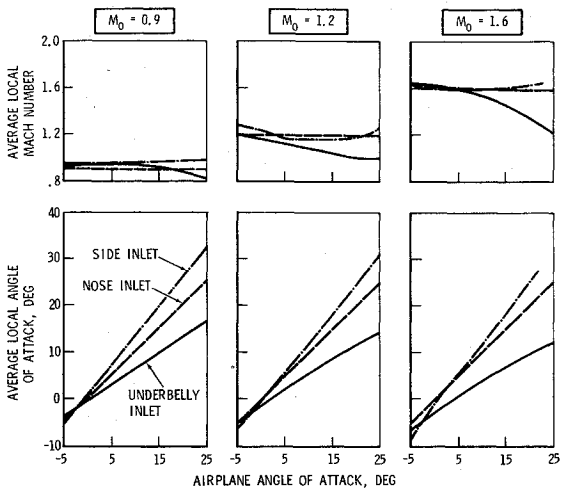

Fig.5 Advantage of underbelly inlet location in terms of local Mach no. and flow angularity.

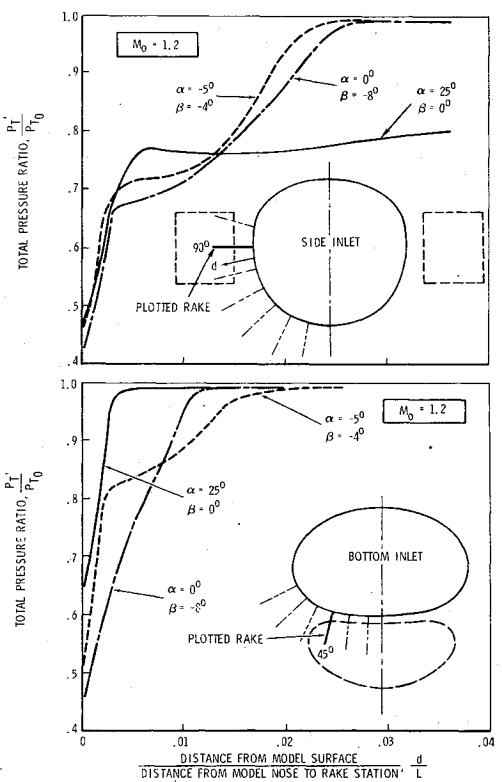

Fig.6 Advantage of underbelly inlet in terms of boundary-layer behavior.

growth ($M > 2.0$). The duct at the forward end of the aft duct assembly was sized to accommodate, as a minimum, a 10% growth in engine airflow.

Inlet-Type Selection

The inlet selection process included trade studies of a normal-shock inlet, and other inlet types designed for more efficient operation at supersonic speeds. A summary of the trade-study results is given in Table 1. The performances of a Mach 2.0 design fixed-compression-surface inlet and a Mach 2.2 design variable-geometry inlet are shown relative to the normal-shock inlet for parameters associated with a typical long-range air-superiority mission. The Mach 2.0 fixed-geometry inlet shows no payoff in the air-combat arena, with a significant penalty in acceleration time and Mach 1.2 turn rate ($\dot{\theta}$) due to the increased weight and drag of the larger inlet. Also, this inlet requires a bypass system for inlet and engine airflow matching at supersonic speeds. The Mach 2.2 variable-geometry inlet also results in turn-rate and acceleration-time penalties due to increased weight and drag, and only shows an improvement in Mach 1.6 specific excess power (P_s). These studies showed conclusively that the simple normal-shock inlet is the optimum inlet for the YF-16 from the standpoint of airplane performance, and would have been the selected design even if low cost were not a design objective.

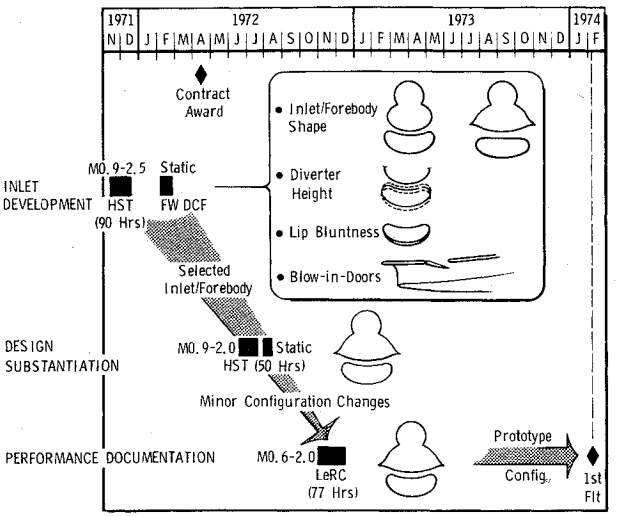

Fig. 7 Inlet development test program.

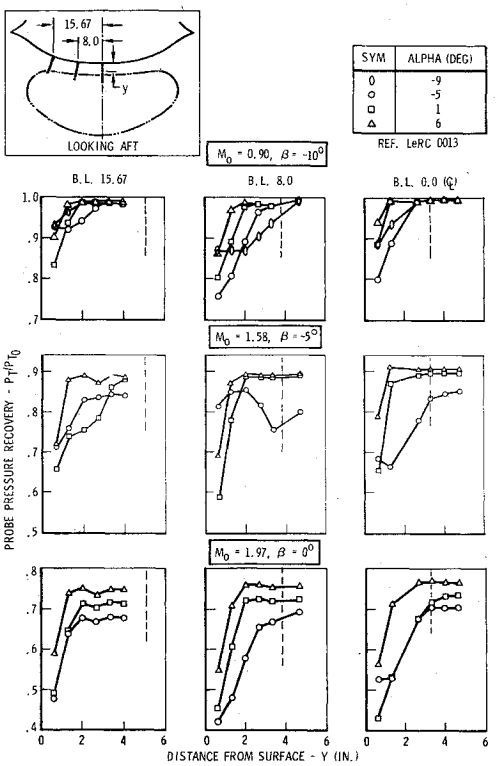

Fig.8 Fuselage boundary-layer total pressure profiles.

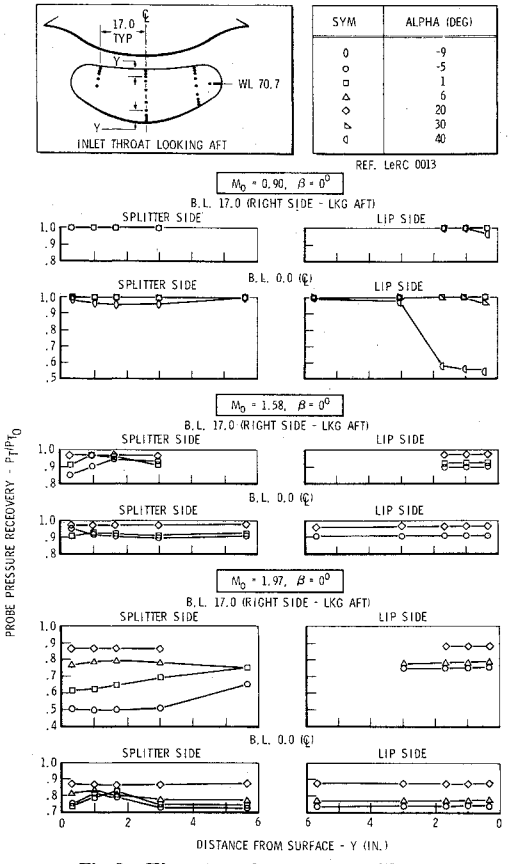

Fig.9 Throat total pressure profiles.

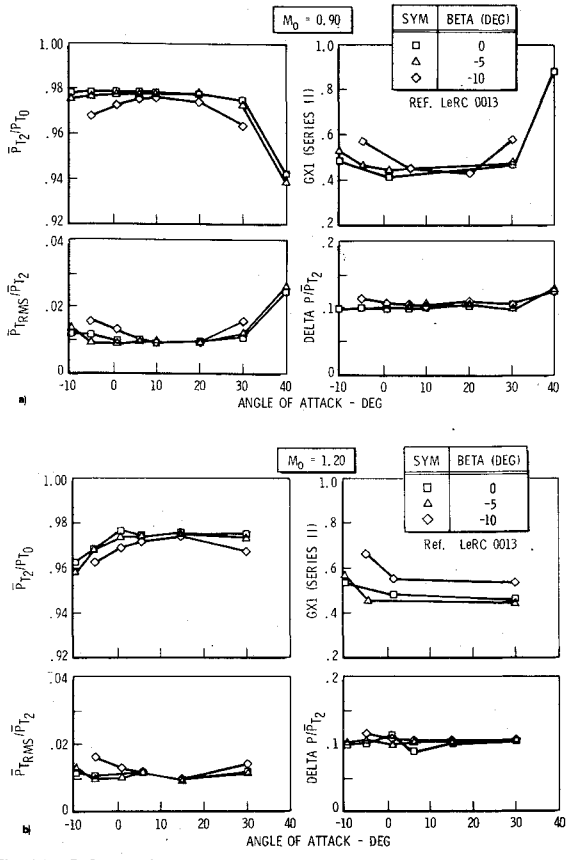

Fig.11 Inlet performance – transonic: a) $M_0 = 0.90$; b) $M_0 = 1.20$.

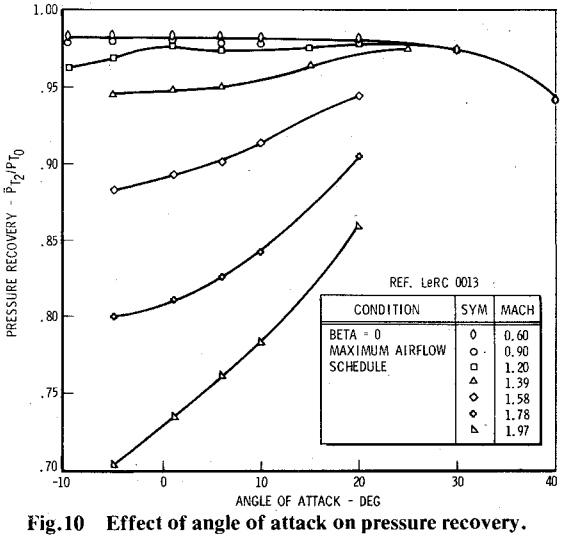

Fig.10 Effect of angle of attack on pressure recovery.

Benefit of Fuselage Shielding

Locating the inlet in the protective flowfield of the forward fuselage significantly enhances the maneuver potential of the aircraft. The airplane forebody is a powerful flow straightener, which is significant in maintaining high inlet pressure recovery and low distortion at high angles of attack. This is illustrated in Fig. 5, where average flowfield properties of local Mach number and flow angularity relative to the inlet are shown for a side inlet, a nose inlet (freestream), and an underbelly inlet location.[1] The underbelly inlet data are for a forebody similar in shape to the YF-16.[1]

The flow straightening provided by the under-fuselage location minimizes the required cowl lip bluntness (and thus inlet size) to achieve high airplane angle of attack without cowl lip flow separation. If the side or nose locations were used, the inlet capture area and lip bluntness would need to be increased, which would result in higher inlet spillage drag and increased inlet weight.

The precompression (reduced local Mach number) at supersonic speeds for the under-fuselage location also results in an increase in inlet total pressure recovery with increases in angle of attack, which improves maneuverability at supersonic speeds. This effect is significant for Mach numbers greater than 1.2. Wind-tunnel-test results of the YF-16 which show this effect are presented subsequently (in Fig. 10, to be cited later).

The under-fuselage inlet location also offers a more favorable boundary-layer condition at high angle of attack than does the side inlet arrangement, as illustrated in Fig.6. The thinner boundary layer for the under-fuselage configuration allows a smaller diverter height (lower diverter drag) and precludes ingestion of the low-energy fuselage boundary-layer air at high angle of attack. Additional boundary-layer data from YF-16 model tests are presented subsequently (in Fig. 8, to be cited later), and confirm that the boundary layer on the bottom of the fuselage is well-behaved over the full angle-of-attack range with no low-energy air entering the inlet.

Inlet Development Program

The basic vehicle for inlet development and performance documentation was a 1/6.67-scale composite forebody/inlet wind-tunnel model. It was equipped with a remotely variable mass-flow plug and a 40-probe steady-state and high-response (0-5000 Hz) compressor-face rake for defining inlet total pressure recovery and distortion. The model also was instrumented with static and total pressure instrumentation for defining the inlet flowfield, fuselage boundary-layer thickness, diverter-channel flowfield, inlet throat-plane pressure recovery and distortion, and subsonic duct performance. The inlet development test program, which consisted basically of three tests, is described in Fig. 7.

The primary configuration variations in the first high-speed test were inlet shape, diverter height, and cowl lip bluntness. The inlet shape selected for subsequent testing was a result of an integration of the best design features from the two inlet shapes shown in Fig. 7 and the forebody configuration selected from force model tests. Diverter height was varied and selected to provide stable operation at all engine airflows and maneuver conditions. Lip bluntness was increased to reduce lip flow separation inside the inlet up to 30° angle of attack. The first static test, in the Fort Worth Duct Calibration Facility, established basic blow-in-door geometry and area. The second test was primarily a design substantiation test of the selected airplane configuration. Only minor configuration differences existed between the second high-speed test and the test at NASA/LeRC.

Performance Summary

A systematic definition of the quality of flow ahead of the inlet, at the inlet throat plane and, finally, at the simulated engine compressor face has resulted in an inlet design that meets the performance and compatibility requirements defined at the outset of the prototype development program. The inlet model data presented are primarily from the NASA/LeRC tests previously described. Inlet spillage drag was determined by tests on conventional, full-airplane force models rather than by highly sophisticated and expensive special-purpose modeling techniques.

Flowfield

The YF-16 fuselage boundary-layer characteristics 5 in. ahead of the splitter-plate leading edge are shown in Fig. 8. These data were obtained with the splitter and diverter in place, but with the inlet cowl removed, so that the inlet shock system would not affect the probe readings. The dashed lines on the plots of Fig. 8 represent the position of the splitter plate (actual airplane position) relative to the fuselage, and show that virtually no low-energy boundary-layer air would be entering the inlet. The difference between the wind tunnel (LeRC 8-by 6-ft tunnel) and flight Reynolds number (where the reference flight altitude is 50,000 ft) gives a theoretical difference in fuselage boundary-layer thickness of about 0.3 in. full scale, which provides even more margin than that shown.

The characteristics of the flow at the inlet throat plane, with the operating inlet in place, are summarized in Fig. 9. These data were obtained with the inlet throttled to correspond to the maximum engine airflow schedule (Fig.2). At Mach 0.9 the total pressures are very uniform (no distortion), except at 40° angle-of-attack, where some lower cowl lip flow separation is evident. At Mach 1.58 the profiles are very uniform at all angles of attack. There is virtually no flow separation on the splitter side of the inlet due to the inlet normal shock interacting with the splitter boundary layer. At Mach 1.97. some non-uniformity exists at B.L. 17 at very low (1°) and negative (−5°) angles of attack because of shock/boundary-layer interaction on the splitter plate, but the long subsonic duct attenuates this distortion at the engine compressor face. The effect of reducing inlet airflow is to further decrease the amount of distortion at the throat plane at all conditions.

Pressure Recovery

Inlet performance in terms of total-pressure recovery is summarized in Fig. 10. Data from the NASA/LeRC tests showed little effect of varying engine airflow at a nominal 1-*g* flight attitude of 1° α and 0° β. The effect of angle of attack on total-pressure recovery from the LeRC tests (Fig. 10) shows the benefit of the underbelly inlet location in terms of maintaining high thrust during high-*g* maneuvers. Level-flight pressure recovery is maintained up to 30° α at subsonic speeds, and an increase in pressure recovery with angle of attack occurs at supersonic speeds.

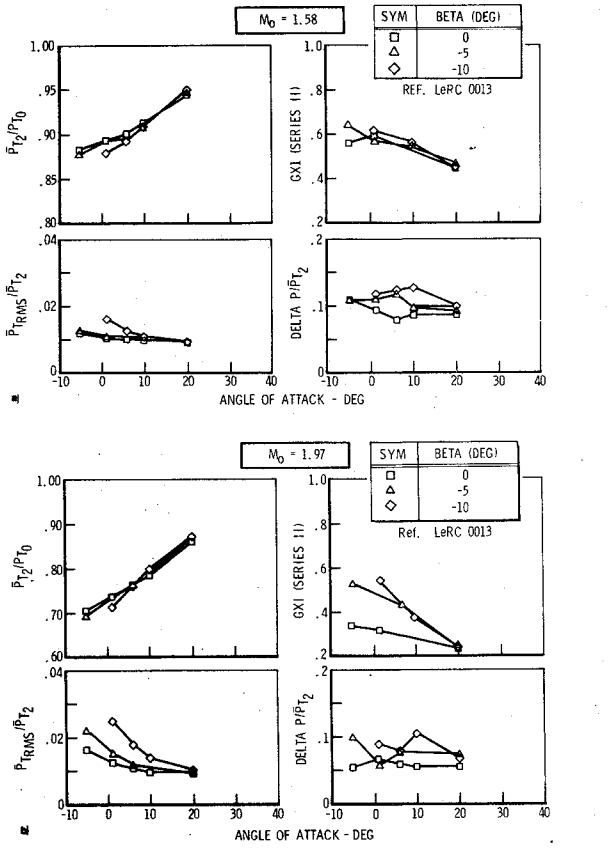

Fig.12 Inlet performance – supersonic; a) $M_0 = 1.58$; b) $M_0 = 1.97$.

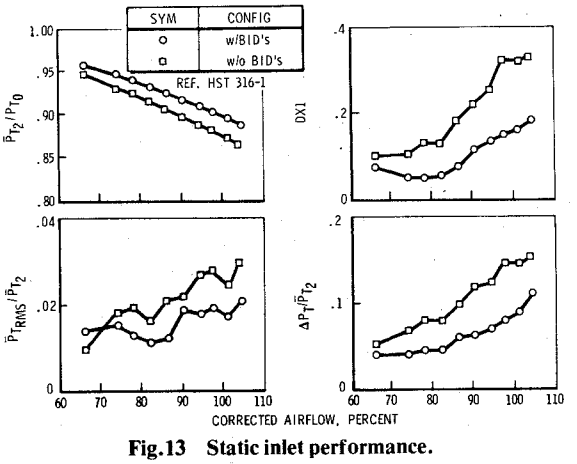

Fig.13 Static inlet performance.

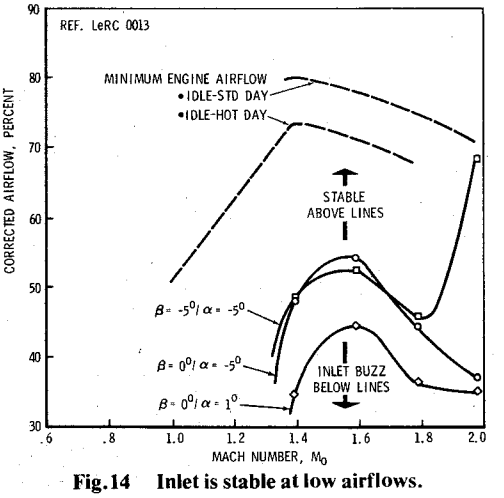

Fig.14 Inlet is stable at low airflows.

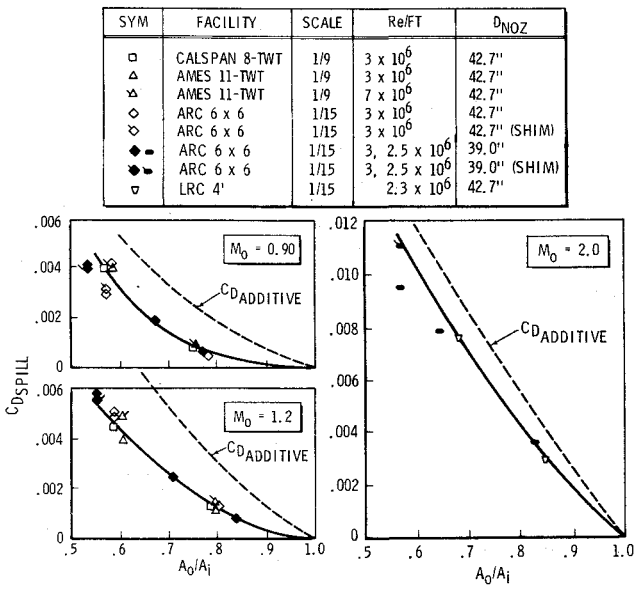

Fig.15 Inlet spillage drag from force model data.

Distortion and Turbulence

Inlet performance in terms of average compressor-face pressure recovery, turbulence, and distortion is summarized in Fig. 11 for Mach 0.9 and 1.2 and in Fig. 12 for Mach 1.58 and 1.97. The distortion parameter GX1 was used to make a preliminary assessment of inlet/engine compatibility and to screeen (select) points with which to perform a rigorous engine stability audit. GX1 is an estimate, based on a correlation of YF-16 steady-state distortion, turbulence, and instantaneous distortion data, of the maximum instantaneous fan distortion index (KA2) divided by the limiting value for the engine, as defined by P&WA. The turbulence parameter $\overline{P_{T_{rms}}}/\overline{P_{T_2}}$ is the average root-mean-square value of fluctuating total pressure as measured by 20 high-response transducers normalized to the average compressor-face steady-state total pressure. Delta $P/\overline{P_{T_2}}$ is the conventional steady-state distortion parameter, $(P_{t_{max}}-P_{t_{min}})/P_{t_{avg}}$. As can be seen, the YF-16 inlet shows very good performance and stability characteristics throughout the airplane maneuver envelope.

The performance of the inlet at sea-level static conditions with and without cowl blow-in-doors is summarized in Fig. 13. In this figure, the distortion parameter DX1 is the fan distortion index (KA2), based on steady-state instrumentation, divided by the estimated limiting instantaneous value. The improvement in inlet performance with blow-in-doors led to their incorporation on the prototype airplance as insurance against having inlet/engine compatibility problems during the prototype flight test program and with flight test engines.

Low-Airflow Stability

Inlet low-airflow stability has been demonstrated to well below the minimum engine airflow limits given in Fig. 2. During the NASA/LeRC test, the inlet was throttled to the "buzz" limit, or, in the case where no buzz was encountered, to essentially zero flow for all α and β combinations tested. The points for which an inlet buzz limit was determined are shown in Fig. 14. At all other points within the operating envelope of the airplane the inlet was completely stable. This range of stability precluded the need for a design and cost compromising bypass system for the YF-16.

Spillage Drag

Performance of the inlet in terms of spillage drag is shown in Fig. 15. These data are from 1/9-scale and 1/15-scale flow-through force-model tests, where inlet capture-area ratio was varied by changing the nozzle exit area. In these tests, care was exercised not to change the aft-end drag when changing nozzle exit area to prevent contaminating the spillage drag indications. Several nozzle diameters were used in these tests, and, since no change in indicated spillage drag occurs with the difference nozzle diameters, it appears that aft-end drag changes indeed have not influenced the spillage drag.

From these tests no significant effect of Reynolds number could be isolated; however, some effect of model scale is evident. The larger 1/9-scale data were favored in the establishment of airplane performance predictions. These data show that significant lip suction exists, even at supersonic speeds. The additive drag shown is simple open-nose inlet additive drag, which should approximate the additive drag of the YF-16 inlet closely.

Conclusions

The single, fixed-geometry, normal-shock inlet design, located in the protective flowfield of the fuselage nose, provides and integrated inlet/airframe configuration that meets all of the performance requirements of the air-combat fighter at minimum weight and cost. Outstanding performance and maneuverability in the primary air-combat arena (Mach 0.6 to 1.6) and a Mach 2.0 capability have been achieved. Indeed, this inlet design optimizes rather than compromises airplane performance in the air-combat arena.

Inlet performance predictions were met and inlet/engine compatibility was achieved by 1) thoroughly mapping the flowfield at the inlet face; 2) providing an adequate diverter height to preclude ingestion of low-energy boundary-layer air into the inlet at any Mach number, α, β, or engine airflow; 3) providing a relatively short splitter plate to minimize boundary-layer buildup and shock/boundary-layer interaction on the splitter; 4) providing a long ($L/D=5.4$) subsonic duct with controlled lines and area distribution; and finally 5) providing a blunt lower cowl lip to forestall lip separation to very high angles of attack ($>30°$).

The underbelly inlet location enhances maneuverability by providing no degradation in pressure recovery to 30° α and stable operation to 40° α subsonically, with an increase in pressure recovery with α at supersonic speeds. Compressor-face turbulence and distortion parameters, calculated from model pressure data, show compatible inlet/engine operation throughout the flight and maneuver envelope of the airplane when compared to estimated limit values as defined by the engine manufacturer.

Spillage drag tests on full-airplane force models provide a known level of inlet spillage drag, which includes all forces due to inlet spillage acting on the airplane. The inlet exhibits significant lip suction even at supersonic speeds.

References

[1] Cawthon, J.A., Crosthwait, E.L., and Truax, P.P., "Supersonic Inlet Design and Airframe-Inlet Integration Program (Project Tailor – Mate), Volume II Forebody Flow Field Investigation," AFFDL-TR-71-124, Vol. II, Air Force Flight Dynamics Laboratory, Wright-Patterson Air Force Base, Ohio, May 1973.